Organic & Biomolecular Chemistry

Cite this: *Org. Biomol. Chem.*, 2012, **10**, 3321

www.rsc.org/obc

**PAPER**

# Dynamic photo-control of kinesin on a photoisomerizable monolayer – hydrolysis rate of ATP and motility of microtubules depending on the terminal group†

**M. K. Abdul Rahim, Takashi Kamei and Nobuyuki Tamaoki***

***Received 23rd December 2011, Accepted 19th February 2012***
**DOI: 10.1039/c2ob07167c**

The reversibly and repeatedly altered gliding motility of microtubules driven by kinesin on the photoresponsive monolayer surface is studied. It was confirmed that an azobenzene monolayer surface needs to have free amino terminal groups for the successful dynamic control of the motility of microtubule. The surface of the azobenzene monolayer with terminal amino groups can dynamically control the ATP hydrolysis activity of kinesin which resulted in the change in motility of the microtubules.



## Introduction

The regulation of nano assembly devices and molecular machines using biomolecular motors as promising components is one of the hot topics in nanotechnology and bio-engineering.[1–9] Kinesins are prominent motor proteins associated with microtubules, which play a central role in both structural and biological functions of the cells.[10–12] The fundamental role of kinesin is to actively distribute the intracellular materials like organelles, vesicles, chromosomes along the microtubules[13,14] and to drive the cell division process by converting the chemical energy of adenosine triphosphate (ATP) into mechanical energy with the positional movement towards the fast polymerizing plus ends of microtubules.[15–17] Each kinesin molecule has two "heads", a 50 nm long semi-flexible coiled-coil region which binds to microtubules and hydrolyses ATP and a "tail", which is thought to bind to the cargo.[18] Among the molecular motors, the kinesin–microtubule system is used widely for developing nanoscale biodevices, because the motility can be regenerated on a surface comparatively easily. In the common *in vitro* construction of the kinesin–microtubule system, the kinesin are adsorbed onto a surface such as glass and microtubules are able to glide across the kinesin coated glass surface.[14] The kinesin–microtubule system has other advantages such as its small size, and the linear movement of single kinesin along the microtubule compared to other molecular motor proteins.[19,20]

The ability to reversibly control the speed of microtubule gliding and the direction of movement on the surface of kinesin by external stimuli would greatly improve the sophistication of nano devices. Several methodologies have been used for the artificial control of microtubule function which includes micro-lithographic tracks,[21,22] electric and magnetic fields,[23] anti-bodies[24] and so on. When considering the biodevices of the future, photochemical energy inputs offer advantages compared to chemical energy inputs because (i) light does not generate waste products; (ii) it can be switched on/off easily and rapidly; (iii) photons, besides supplying the energy to the system, can also be useful to "read" the state of the system and thus to control and monitor the operation of the machine *etc*. Higuchi *et al*.[25] used the caged ATP as photo-controlled switch, because their inactive caged states (OFF state of motility) can be converted to active uncaged states (ON state of motility) by UV light irradiation. Another group successfully used the photolysis of caged ATP to develop molecular shuttles on engineered kinesin tracks.[26] On the other hand Tatsu *et al.* demonstrated the switching of kinesin's activity from the ON state to the OFF state by the photolysis of caged peptide derived from the kinesin C-terminus domain working as an inhibitor.[27] In that study, they successfully demonstrated an 80% reduction of the initial gliding velocity of microtubules on the kinesin surface after the photochemical deprotection of the *o*-nitrobenzyl protecting group on the caged peptide. All these methods can either trigger the initiation of the movement or cessation of the microtubule motility. To design the more useful nanoscale biodevices, it is important that the system should provide ON and OFF switching of gliding motility at any desired time and at any desired position in space. To the best of our knowledge the light controlled reversible and repeated switching of microtubule motility was demonstrated only by our group.[28]

*Research Institute for Electronic Science, Hokkaido University, N20, W10, Kita-ku, 001-0020, Sapporo, Hokkaido, Japan. E-mail: tamaoki@es.hokudai.ac.jp; Fax: +81 11 706 9357; Tel: +81 11 706 9356*

†Electronic supplementary information (ESI) available. See DOI: 10.1039/c2ob07167c

We reported the reversible and repeated regulation of the motility of microtubule by the photoisomerization of the underlying monolayer using two different wavelengths of light.[28] For the fabrication of such photoresponsive monolayer, we employed a derivative of azobenzene; one of the most studied photochromic compounds[29–33] due to its strong photo-switching effect, reversibility and simplicity of incorporation,[34] with a triethoxy silane group which react with the glass surface to be anchored and a lysine group which can interact with motor proteins. Using this approach, we described the reversible and repeated control of the gliding velocity of microtubules driven by kinesin on the azobenzene monolayer (with a maximum of 15% difference in velocity) upon irradiation with UV and visible light.[35] In this paper we are reporting the generality of the system in the repeated regulation of fast and slow modes of microtubule gliding motility by devising a series of surface of azobenzene monolayers with various terminal groups. We also propose a mechanism that accounts for the changes in the velocity of microtubule when the photoresponsive monolayer surface is isomerized between *E* and *Z* states upon irradiation of different wavelengths of light. We believe that the method developed here should be applicable in forthcoming nanoscale biodevices based on the kinesin–microtubule system.

## Experimental

### Materials

Unless otherwise noted, all reagents including solvents were obtained from major commercial suppliers such as TCI, Sigma-Aldrich and Wako used directly without further purification. DMF was routinely dried and/or distilled prior to use and stored over molecular sieves (4A). Column chromatography was performed with silica gel (63–210 μm).

### General methods, instrumentation and measurements

$^1$H NMR spectra were recorded at 400 MHz using TMS as an internal standard. Matrix-Assisted Laser Desorption Ionization Time-Of-Flight Mass Spectrometry (MALDI-TOF MS) was performed on an applied Biosystems Voyager-DE pro instrument with positive-ion mode. Absorption spectra were recorded on an Agilent 8453 spectrophotometer and also a Hitachi U-3100 absorption spectrophotometer. Photo-isomerization studies were conducted using a mercury–xenon lamp (Hamamatsu Photonics K.K. 200 W) after passage through appropriate filters (366 or 440 or >500 nm).

Microtubules motility assay were carried out using fluorescence microscope (Olympus BX50 or Nikon TEi) equipped with a high NA objective lens (100×, 1.30 NA for Olympus BX50 and 100×, 1.45 NA for Nikon TEi) and the fluorescence image was recorded with appropriate filters (Chroma) to remove the excitation light, back-illuminate electron-cooled CCD camera (EM9100-12, HAMAMATSU), and the image processing system AQUACOSMOS (HAMAMATSU). Both were performed at room temperature (22 °C).

### Synthesis

The synthetic route to compounds **1b′–e′** and **2a** are illustrated in Schemes 1–3 and compound **2b** was commercially purchased. Synthetic details for **1a′** were reported in our previous paper. Detailed synthetic procedures for **1b′–e′** and **2a** are described below. Compounds **4** and **5** were prepared according to the literature.[36]

**Compound 7.** Hydroxybenzotriazole (115 mg, 0.848 mmol) and *N*,*N*′-dicyclohexylcarbodiimide (175 mg, 0.848 mmol) were added under an argon atmosphere to a solution of Boc-Arg-

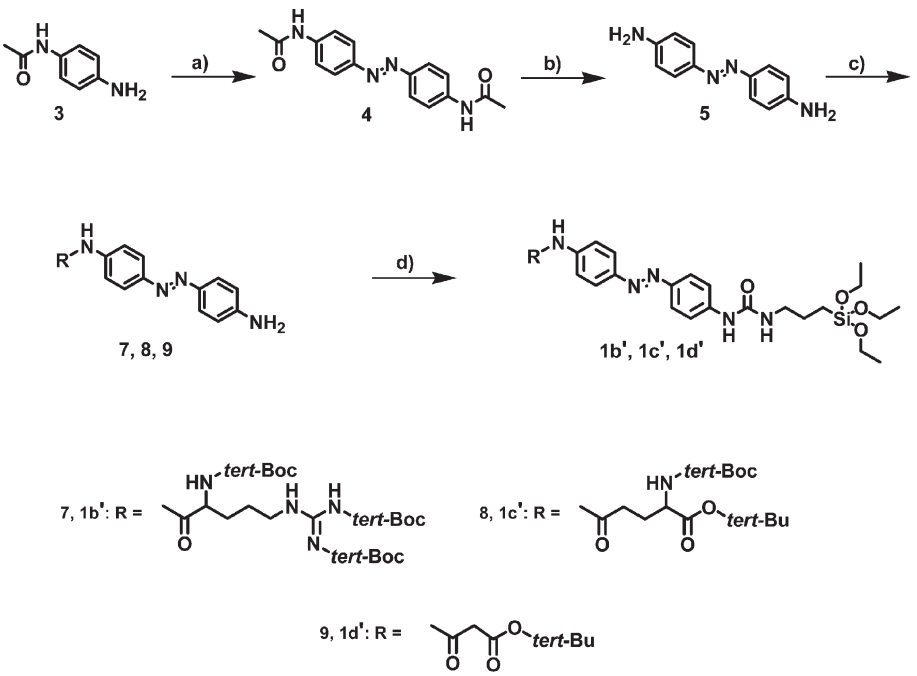


**Scheme 1** (a) $NaBO_3$, $H_3BO_3$, HOAc, HCl, MeOH, 60 °C. (b) NaOH. (c) For **7**, **1b′** = Boc–Arg–$(Boc)_2$–OH, for **8**, **1c′** = Boc–Glu–(OtBu)–OH and for **9**, **1d′** = mono-*tert*-butyl malonate, DCC, HOBt, DMF. (d) OCN–$(CH_2)_3$–Si–$(OEt)_3$, THF.

 

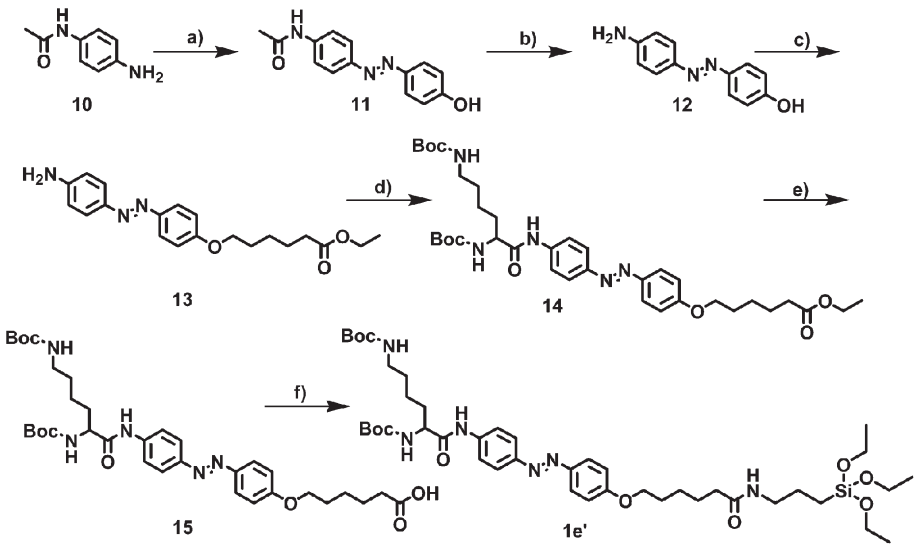


**Scheme 2** (a) HCl, $H_2O$, $NaNO_2$, NaOH, PhOH, 0–2 °C. (b) 10% NaOH, reflux 2 h. (c) Br–$(CH_2)_5$–COOEt, $K_2CO_3$, $(CH_3)_2CO$, 50–60 °C. (d) Boc–Lys–(Boc)–OH·DCHA, DCC, HOBt, DMF. (e) Dioxane, 1 M aq. KOH. (f) OCN–$(CH_2)_3$–Si–$(OEt)_3$, THF.

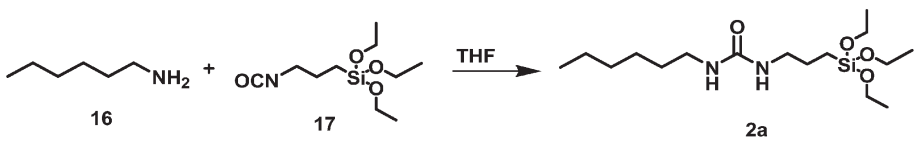


**Scheme 3** Synthetic scheme of compound **2a**.

$(Boc)_2$-OH (268 mg, 0.565 mmol) in dry DMF (5 mL) at room temperature. After 1 h, 4,4′-diaminoazobenzene (**5**) (150 mg, 0.707 mmol) was added and the mixture was stirred at room temperature overnight. The mixture was then diluted with brine and was extracted with ethyl acetate (EtOAc); the combined extracts were dried ($MgSO_4$) and the solvent was removed under reduced pressure. The residue was purified by column chromatography (eluent: dichloromethane (DCM)–EtOAc). Yield: 41%. $^1$H NMR (400 MHz, $CDCl_3$): $\delta$ = 1.40 (s, 9H), 1.51 (d, $J$ = 4 Hz, 18H), 1.65–1.71 (m, 2H), 1.82–1.95 (m, 4H), 3.81 (m, 1H), 4.07 (br, 2H), 4.55 (m, 1H), 5.95 (q, $J$ = 4 Hz, 1H), 6.72 (d, $J$ = 8 Hz, 2H), 7.61 (d, $J$ = 8 Hz, 2H), 7.77 (d, $J$ = 8 Hz, 2H), 7.82 (d, $J$ = 8 Hz, 2H), 9.19 (br, 1H), 9.29 (br, 1H). MS (MALDI): Calculated for $C_{33}H_{48}N_8O_7$ $[M + H]^+$ $m/z$ 669.36; found $m/z$ 669.66.

**Compound 1b′.** Triethoxysilylpropyl isocyanate (62 mg, 0.251 mmol) was added to a solution of **7** (252 mg, 0.377 mmol) in anhydrous tetrahydrofuran (THF) (3 mL). The mixture was refluxed under $N_2$ atmosphere until the completion of the reaction. The residue was washed with copious amounts of hexane and was then dried under vacuum. Yield: 71%. $^1$H NMR (400 MHz, $CDCl_3$): $\delta$ = 0.61 (t, $J$ = 8 Hz, 2H), 1.17 (t, $J$ = 8 Hz, 9H), 1.43 (d, $J$ = 4 Hz, 18H), 1.52 (s, 9H), 1.63 (m, 2H), 1.77 (m, 2H), 1.89 (m, 2H), 2.89 (q, $J$ = 4 Hz, 2H), 3.23 (q, $J$ = 4 Hz, 2H), 3.79 (q, $J$ = 8 Hz, 6H), 3.96 (m, 1H), 4.34 (br, 1H), 5.97 (q, $J$ = 4 Hz, 1H), 6.33 (m, 2H), 7.67 (d, $J$ = 8 Hz, 2H), 7.81 (d, $J$ = 4 Hz, 2H), 7.83 (d, $J$ = 4 Hz, 2H), 7.85 (d, $J$ = 4 Hz, 2H), 8.27 (s; urea H atom close to aryl, 1H), 9.26 (br, 1H). $^{13}$C-NMR (400 MHz, $CDCl_3$): $\delta$ = 171.10, 170.83, 161.17, 155.75, 155.15, 154.80, 149.29, 148.18, 141.84, 141.70, 124.07, 123.55, 120.14, 119.34, 82.96, 82.33, 80.00, 58.52, 55.63, 48.47, 42.70, 28.43, 28.09, 24.99, 23.47, 22.99, 18.31, 7.66. MS (MALDI): Calculated for $C_{43}H_{69}N_9O_{11}Si$ $[M + H]^+$ $m/z$ 917.48; found $m/z$ 917.43.

**Compound 8.** Hydroxybenzotriazole (115 mg, 0.848 mmol) and $N,N'$-dicyclohexylcarbodiimide (175 mg, 0.848 mmol) were added under an argon atmosphere to a solution of Boc-Glu-(O*t*Bu)-OH (172 mg, 0.565 mmol) in dry DMF (5 mL) at room temperature. 4,4′-Diaminoazobenzene (**5**) (150 mg, 0.707 mmol) was added after 1 h and the mixture was stirred at room temperature overnight. The mixture was then diluted with brine and was extracted with ethyl acetate (EtOAc); the combined extracts were dried ($MgSO_4$) and the solvent was removed under reduced pressure. The residue was purified by column chromatography (eluent: DCM–EtOAc). Yield: 43%. $^1$H NMR (400 MHz, $CDCl_3$): $\delta$ = 1.45 (d, $J$ = 8 Hz, 18H), 1.59–1.63 (m, 2H), 2.45–2.49 (t, $J$ = 8 Hz, 2H), 4.09 (br, 2H), 4.24 (br, 1H), 5.4 (q, $J$ = 4 Hz, 1H), 6.71 (d, $J$ = 8 Hz, 2H), 7.74 (d, $J$ = 8 Hz, 2H), 7.77 (d, $J$ = 8 Hz, 2H), 7.83 (d, $J$ = 8 Hz, 2H), 9.12 (Br, 1H). MS (MALDI): Calculated for $C_{26}H_{35}N_5O_5$ $[M + H]^+$ $m/z$ 498.26; found $m/z$ 498.36.

**Compound 1c′.** Triethoxysilylpropyl isocyanate (76.6 mg, 0.31 mmol) was added to a solution of **8** (235 mg, 0.465 mmol) in anhydrous tetrahydrofuran (THF) (3 mL). The mixture was refluxed under $N_2$ atmosphere until the reaction was completed.

The residue was washed with copious amounts of hexane and was then dried under vacuum. Yield: 79%. $^1$H NMR (400 MHz, $CDCl_3$): $\delta$ = 0.65 (t, $J$ = 8 Hz, 2H), 1.20 (t, $J$ = 8 Hz, 9H), 1.46 (d, $J$ = 8 Hz, 18H), 1.64 (m, 2H), 2.23–2.33 (m, 2H), 2.47–2.51 (t, $J$ = 8 Hz, 2H), 3.26 (q, $J$ = 4 Hz, 2H), 3.79 (q, $J$ = 6 Hz, 6H), 4.24 (br, 1H), 5.39 (br, 1H), 5.42 (q, $J$ = 4 Hz, 1H), 7.06 (br, 1H), 7.44 (d, $J$ = 8 Hz, 2H), 7.73 (d, $J$ = 8 Hz, 2H), 7.79 (d, $J$ = 8 Hz, 2H), 7.84 (d, $J$ = 8 Hz, 2H), 9.24 (s; urea H atom close to aryl, 1H). $^{13}$C-NMR (400 MHz, $CDCl_3$): $\delta$ = 171.21, 155.31, 149.63, 149.02, 142.22, 141.68, 124.00, 123.70, 119.94, 119.42, 82.94, 80.71, 58.53, 53.20, 42.68, 34.25, 31.00, 28.35, 27.96, 25.80, 23.48, 22.65, 18.33, 7.62. MS (MALDI): Calculated for $C_{36}H_{56}N_6O_9Si$ $[M + H]^+$ $m/z$ 745.39; found $m/z$ 745.43.

**Compound 9.** Hydroxybenzotriazole (191 mg, 1.4 mmol) and *N*,*N*′-dicyclohexylcarbodiimide (292 mg, 1.4 mmol) were added under an argon atmosphere to a solution of mono-tert-butyl malonate (151 mg, 0.94 mmol) in dry DMF (3 mL) at room temperature. After 1 h, 4,4′-diaminoazobenzene (**5**) (250 mg, 1.18 mmol) was added and the mixture was stirred at room temperature overnight. The mixture was then diluted with brine and was extracted with ethyl acetate (EtOAc); the combined extracts were dried ($MgSO_4$) and the solvent was removed under reduced pressure. The residue was purified through column chromatography (eluent: DCM–EtOAc). Yield: 46%. $^1$H NMR (400 MHz, $CDCl_3$): $\delta$ = 1.45 (s, 9H), 3.34 (s, 2H), 3.97 (br, 2H), 6.64 (d, $J$ = 8 Hz, 2H), 7.62 (d, $J$ = 8 Hz, 2H), 7.70 (d, $J$ = 8 Hz, 2H), 7.76 (d, $J$ = 8 Hz, 2H), 9.50 (br, 1H). MS (MALDI): Calculated for $C_{19}H_{22}N_4O_3$ $[M + H]^+$ $m/z$ 355.17; found $m/z$ 355.08.

**Compound 1d′.** Triethoxysilylpropyl isocyanate (104 mg, 0.42 mmol) was added to a solution of **9** (150 mg, 0.42 mmol) in anhydrous tetrahydrofuran (THF) (3 mL). The mixture was refluxed under $N_2$ atmosphere until the completion of the reaction. The residue was washed with copious amounts of hexane and was then dried under vacuum. Yield: 83%. $^1$H NMR (400 MHz, $CDCl_3$): $\delta$ = 0.64 (t, $J$ = 8 Hz, 2H), 1.19 (t, $J$ = 8 Hz, 9H), 1.52 (s, 9H), 1.60–1.69 (m, 2H), 3.23 (q, $J$ = 4 Hz, 2H), 3.44 (s, 2H), 3.78 (q, $J$ = 6 Hz, 6H), 5.72 (m, 2H), 7.40 (d, $J$ = 8 Hz, 2H), 7.55 (br, 1H), 7.63 (d, $J$ = 4 Hz, 2H), 7.76 (d, $J$ = 4 Hz, 2H), 7.80 (d, $J$ = 4 Hz, 2H), 9.64 (s; urea H atom close to aryl, 1H). $^{13}$C-NMR (400 MHz, $CDCl_3$): $\delta$ = 169.08, 164.07, 155.60, 149.44, 147.87, 142.16, 139.24, 124.02, 123.65, 120.55, 119.13, 83.36, 58.48, 53.45, 42.68, 28.04, 18.31, 14.20, 7.66. MS (MALDI): Calculated for $C_{29}H_{43}N_5O_7Si$ $[M + H]^+$ $m/z$ 602.29; found $m/z$ 602.39.

Compounds **11** and **12** were prepared according to the literature.[37]

**Compound 13.** 4-(4′-Hydroxyphenylazo)aniline (**12**) (2.10 g, 10 mmol), 6-bromo-hexanoic acid ethyl ester (3.4 g, 15.2 mmol) and potassium carbonate (2.8 g, 38 mmol) was dissolved in acetone (60 mL) and the mixture was refluxed for 12 hours under argon atmosphere. The mixture was then diluted with brine and was extracted with ethyl acetate (EtOAc); the combined extracts were dried ($MgSO_4$) and the solvent was removed under reduced pressure. The resulting mixture was submitted for silica column chromatography using a mixed solvent (DCM–EtOAc, 9 : 1) and **13** was obtained in 91% yield. $^1$H NMR (400 MHz, $CDCl_3$): $\delta$ = 1.24 (t, $J$ = 6 Hz, 3H), 1.50 (m, 2H), 1.68 (m, 2H), 1.80 (m, 2H), 2.32 (t, $J$ = 8 Hz, 2H), 3.98 (t, $J$ = 8 Hz, 2H), 4.02 (br, 2H), 4.10 (q, $J$ = 8 Hz, 2H), 6.72 (d, $J$ = 8 Hz, 2H), 6.95 (d, $J$ = 8 Hz, 2H), 7.75 (d, $J$ = 8 Hz, 2H), 7.81 (d, $J$ = 8 Hz, 2H). MS (MALDI): Calculated for $C_{20}H_{25}N_3O_3$ $[M + H]^+$ $m/z$ 356.20; found $m/z$ 356.23.

**Compound 14.** HOBt (200 mg, 1.48 mmol), EDC (284 mg, 1.48 mmol) and $Et_3N$ (0.196 μL, 1.4 mmol) were added to a DMF (10 mL) solution of Boc-Lys-(Boc)·DCHA (520 mg, 1.4 mmol) at 0 °C under argon atmosphere. After keeping at 0 °C for 15 minutes and 30 minutes at room temperature, the compound **13** (510 mg, 1.44 mmol) was added and the mixture was stirred overnight at room temperature. The mixture was diluted with brine and was extracted with ethyl acetate, dried over $MgSO_4$ and the solvent was removed under reduced pressure. The residue was purified using column chromatography (DCM–AcOEt mixture as eluents (8 : 2)) and **14** were obtained as yellow powder in 48% yield. $^1$H NMR (400 MHz, $CDCl_3$): $\delta$ = 1.19 (m, 2H), 1.24 (t, $J$ = 6 Hz, 3H), 1.31 (m, 2H), 1.43 (d, $J$ = 8 Hz, 18H), 1.52 (m, 2H), 1.70 (m, 2H), 1.80 (m, 2H), 1.88 (m, 2H), 2.32 (t, $J$ = 6 Hz, 2H), 3.15 (m, 2H), 3.79 (q, $J$ = 8 Hz, 2H), 4.02 (t, $J$ = 6 Hz, 2H), 4.17 (br, 1H), 4.61 (m, 1H), 5.21 (br, 1H), 6.96 (d, $J$ = 12 Hz, 2H), 7.68 (d, $J$ = 8 Hz, 2H), 7.85 (d, $J$ = 4 Hz, 2H), 7.87 (d, $J$ = 4 Hz, 2H), 8.64 (br, 1H). MS (MALDI): Calculated for $C_{36}H_{53}N_5O_8$ $[M + H]^+$ $m/z$ 684.40; found $m/z$ 684.47.

**Compound 15.** 1 M KOH aq. solution (3 mL) was added to a solution of **14** (200 mg, 0.29 mmol) in dioxane (6.0 mL). After stirring for 2 h at room temperature the mixture was neutralized with 2 N $NH_4^+Cl^-$, extracted with AcOEt and was dried over $MgSO_4$. The residue was purified by column chromatography (AcOEt) and **15** was obtained in 47% yield. $^1$H NMR (400 MHz, $CDCl_3$): $\delta$ = 1.24 (m, 2H), 1.45 (d, $J$ = 4 Hz, 18H), 1.50 (m, 2H), 1.68 (m, 2H), 1.81 (m, 2H), 1.86 (m, 2H), 2.03 (m, 2H), 2.33 (t, $J$ = 8 Hz, 2H), 3.09 (m, 2H), 4.02 (t, $J$ = 6 Hz, 2H), 4.05 (br, 1H), 4.65 (m, 1H), 5.21 (br, 1H), 6.96 (d, $J$ = 12 Hz, 2H), 7.68 (d, $J$ = 8 Hz, 2H), 7.85 (d, $J$ = 4 Hz, 2H), 7.87 (d, $J$ = 4 Hz, 2H), 8.65 (br, 1H). MS (MALDI): Calculated for $C_{34}H_{49}N_5O_8$ $[M + H]^+$ $m/z$ 656.34; found $m/z$ 656.36.

**Compound 1e′.** The mixture solution of 100 mg (0.15 mmol) of **15**, 67 mg (0.31 mmol) of (3-aminopropyl) triethoxy silane and 67 mg (0.31 mmol) of dicyclohexylcarbodiimide in DCM (12 mL) was stirred for 2 h under ice cooling. The precipitated dicyclohexylurea was removed by filtration. The filtrate was evaporated under reduced pressure, washed with copious amounts of hexane and was then dried under vacuum affording the product as orange solid. The crude residue **1e′** was used without any further purification. $^1$H NMR (400 MHz, $CDCl_3$): $\delta$ = 0.86 (t, $J$ = 4 Hz, 2H), 1.24 (t, $J$ = 6 Hz, 9H), 1.45 (d, $J$ = 4 Hz, 18H), 1.51–1.61 (m, 10H), 1.68–17.76 (m, 2H), 1.80–1.88 (m, 2H), 1.95 (t, $J$ = 8 Hz, 2H), 2.33 (t, $J$ = 6 Hz, 2H), 3.09 (m, 2H), 3.79 (t, $J$ = 4 Hz, 1H), 4.02 (t, $J$ = 6 Hz, 2H), 4.11 (q, $J$ = 4 Hz, 6H), 4.19 (br, 1H), 4.64 (m, 1H), 5.21 (br, 1H), 6.96 (d, $J$ = 4 Hz, 2H), 7.67 (d, $J$ = 12 Hz, 2H), 7.85 (d, $J$ = 4 Hz, 2H), 7.87 (d, $J$ = 4 Hz, 2H), 8.65 (br, 1H). Yield was 86%. $^{13}$C-NMR (400 MHz, $CDCl_3$): $\delta$ = 172.35, 169.57, 160.27, 155.22, 152.92, 148.04, 145.87, 138.77, 123.49, 122.47, 118.71, 113.58, 79.47, 78.25, 66.88, 58.81, 52.46, 48.60, 47.96, 34.52, 32.83, 31.64,

 

29.88, 27.93, 27.37, 27.25, 25.25, 21.52, 18.35, 17.21, 8.59. MS (MALDI): Calculated for $C_{34}H_{49}N_5O_8$ $[M + H]^+$ *m/z* 859.49; found *m/z* 859.62.

**Compound 2a.** Triethoxysilylpropyl isocyanate (**17**) (2.5 g, 10.1 mmol) was added to a solution of hexylamine (**16**) (1.53 g, 15.18 mmol) in THF (6 mL) and was refluxed for 36 hours under argon atmosphere. After the completion of reaction, the residue was washed with copious amount of hexane and was dried under vacuum. Yield: 78%. $^1$H NMR (400 MHz, $CDCl_3$): $\delta = 0.52$ (t, $J = 12$ Hz, 2H), 0.79 (t, $J = 4$ Hz, 3H), 1.11 (t, $J = 8$ Hz, 9H), 1.20 (m, 4H), 1.37 (m, 2H), 1.50 (m, 2H), 1.78 (m, 2H), 3.05 (m, 4H), 3.71 (q, $J = 6$ Hz, 6H), 5.23 (m, 2H). MS (MALDI): Calculated for $C_{16}H_{36}N_2O_4Si$ $[M + H]^+$ *m/z* 349.24; found *m/z* 349.36.

### Preparation of monolayer

Preparation of monolayer was done by a modification of the methods described elsewhere[38] through the formation of siloxane linkages between **1a–d** or **2a** and the substrate. Glass or quartz plates were purified ultrasonically in acetone, in concentrated nitric acid and aqueous solution of saturated sodium bicarbonate in sequence. Each ultra-sonication was carried out for 10 min and followed by washing with Milli-Q water. After drying at 120 °C for 30 minutes, the plates were dipped in a mixed THF solution containing compound **1a′–e′** along with compound **2a** or **2b** (total concentration: 2 mM) at room temperature for 30 minutes. The modified plates were dried at 120 °C for 30 minutes and washed ultrasonically in THF for 10 minutes and dried again at 120 °C for 30 minutes. The *tert*-Boc protecting groups of **1a′–e′** were removed by dipping the monolayer in a 30% trifluoroacetic acid (TFA) in DCM solution[39] which yielded the target compounds **1a–e**. The quantitative removal of the *tert*-Boc protecting group was verified by the measurements of contact angle before and after deprotection.

### Optical measurements and photoisomerization

For photo-switching the azobenzene **1a′–d′**, samples (in acetonitrile, 22 °C) were irradiated at 366 nm (*trans* to *cis*) and >500 nm (*cis* to *trans*), and **1e′** sample (in DCM, 22 °C) were irradiated with 366 nm (*trans* to *cis*) and 440 nm (*cis* to *trans*) respectively, using a mercury–xenon lamp (Hamamatsu Photonics K.K. 200 W) and band-pass filters (366, >500 and 440 nm). Thermal relaxation of the *cis* to the *trans* isomer was monitored with the same spectrophotometer under dark condition. The absorption spectra of mixed monolayer of **1a–e** incorporated on a quartz plate were recorded with same method and time as in solution, before and after photoirradiation using appropriate band-pass filters (366, >500 and 440 nm) on a Hitachi U-3100 absorption spectrophotometer.

### Contact angle measurements

The sample consisting of the monolayer was placed on a flat surface and water, which is used as the fluid, was dropped on the sample using a syringe. The image of the sample was obtained by adjusting the light and focus of the camera. To confirm the deprotection of *tert*-Boc group, images were taken before and after deprotection, and to study the reversible changes in surface properties upon photoirradiation images were taken before and after 366 nm wavelength light irradiation.

### Proteins preparations

Tubulins were purified from porcine brains through two cycles of polymerization–depolymeraization processes in the presence of a high-molarity PIPES buffer.[40] Microtubules were polymerized using the purified tubulins and labelled with tetramethylrhodamine succinimidyl ester. Kinesin utilized in this research was a recombinant kinesin consist of 573 amino acid residues from N-terminus of a conventional human kinesin. This recombinant kinesin fused with His-tag in the N-terminus (plasmid; pET30b) was expressed in *Escherichia coli* Rosetta (DE3) pLysS and purified by the general method utilizing Ni–NTA–agarose.

### Flow cells

The flow cells were prepared by placing two strips of double-stick tape on a glass slide *ca.* 6–9 mm apart and covered with an 18 × 18 or 22 × 22 mm cover slip consisting of monolayer. The inner volume of the obtained flow cell was *ca.* 10–12 μL. Solutions were pipetted on one side and sucked out on the other side by capillary action using Whatman filter paper or a Kim wipe as shown elsewhere.[41,42]

### Motility assays

For these experiments, a simple protocol using the standard capillary flow technique reported elsewhere for kinesin motility assay with polarity marked taxol microtubules[11] was employed. For all experiment the starting buffer was BRB80 (80 mM PIPES, 2 mM $MgCl_2$, 1 mM EGTA, pH 6.95 with KOH). The azobenzene embedded flow cells were sequentially filled with a standard kinesin solution (0.3069 mg $mL^{-1}$, which is just sufficient for the movement of microtubules) and kept in moist conditions for five minutes. Unbound kinesins were washed out with a solution containing 20 μl of BRB80 assay buffer + 1 mM DTT + 1 mM MgATP + 10 μM taxol. And then a motility buffer consisting of BRB80 and microtubules labelled by tetramethylrhodamine succinimidyl ester were stabilized with taxol (5–10 μm in length). After keeping like this for five minutes, the unbound microtubules were washed out by the assay buffer containing taxol with an added oxygen scavenger system (2-mercaptoethanol: 0.14 M, glucose 20 mM, catalase: 20 μg $ml^{-1}$, glucose oxidase: 100 μg $ml^{-1}$). The flow cells were sealed with immersion oil to prevent evaporation and were transferred to the fluorescence microscope. The translocation of microtubules were monitored and recorded after UV and visible light irradiation.

### ATPase assays

In the presence of azobenzene monolayer and microtubules, the kinesin ATPase activity was measured *via* a simple and sensitive colorimetric assay based on the determination of released

inorganic phosphate ion by an improved malachite green procedure.[43,44] In short, at fixed time intervals, aliquots were removed from the motility assay system and quickly mixed with an equal volume of ice-chilled perchloric acid (PCA) and malachite green reagent. The mixture was kept at 25 °C for 40 minutes and then the absorbance was measured at 630 nm with a Hitachi U-3100 absorption spectrophotometer and concentration of inorganic phosphate (Pi) was determined. Then the same flow cell was irradiated with 366 nm light until the sample reached its photostationary state (PSS). The aliquots at fixed time intervals were removed from the motility assay system and mixed with equal volumes of ice-chilled PCA and malachite green reagent and the same procedure was repeated. In order to know the reversibility, the above procedure was repeated by irradiating the flow cells with visible light.

## Results and discussion

The dynamic control of the motility of microtubule driven by kinesin, upon photo-isomerization of azobenzene monolayer was studied with alkyl silane compounds shown in Chart 1, namely, 3-(triethoxysilyl)propyl urea attached to azobenzene moiety with one lysine (**1a**), arginine (**1b**), glutamic acid (**1c**) or malonic acid residue (**1d**) at the end and a 3-(triethoxysilyl)propyl 6-hydroxyhexanoic amide attached to azobenzene moiety with lysine residue (**1e**) at the end. One of the issues in the synthesis of silane functionalized azobenzene was the difficulty in purifying the final product. Without the purification of the final products,

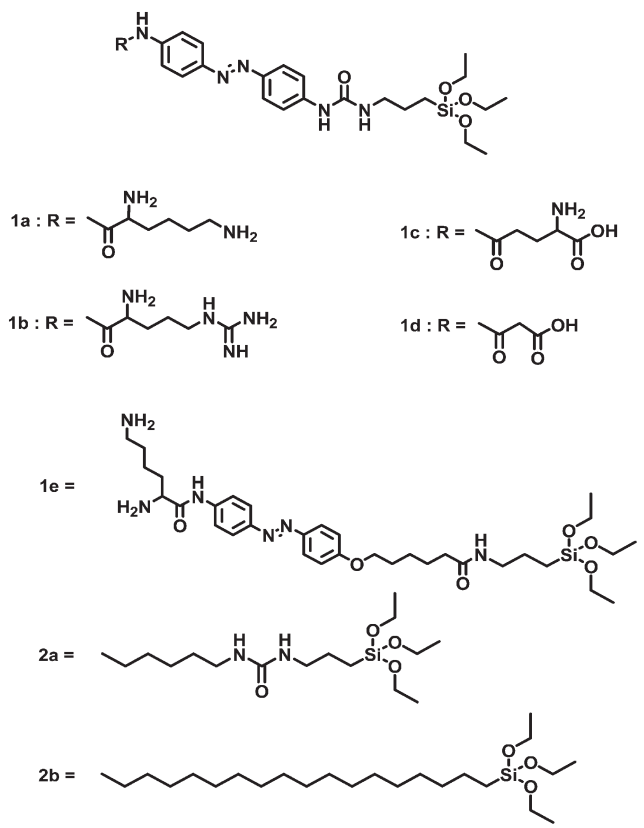


**Chart 1** Chemical structures of photoresponsive azobenzene silane compounds (**1a–e**) along with alkyl silane chains (**2a** and **2b**).

on the basis of HPLC, we estimated 93% purity with unreacted azobenzene starting material as impurity. Since the azobenzene starting material is not reactive towards the glass surface, we did not consider its presence as a problem for monolayer formation.

One of the important parameters for fabrication of dynamic monolayer surfaces is reversibility of switching. Pace *et al.*[45] already reported that steric constraints of tightly packed matrixes can restrict conformational changes, thus hindering isomerization in azobenzene. In order to avoid such hindrance, we prepared a mixed monolayer which can reduce the steric constraints. For compound **1a–d**, we used 90% of non-photo isomerizable compound **2a** for preparing mixed monolayer which forms hydrogen bonding with each other, and for **1e** we used 90% of **2b**. The removal of *tert*-Boc groups on the surface upon TFA treatment is confirmed by the change in the contact angle. The contact angle of monolayer, before release of *tert*-Boc group of **1b′** was 74° and after 4 h treatment with TFA, it is reduced to 66°. The other compounds also show a similar trend for the water contact angle, which is summarized in the table (ESI Table S1†).

Fig. 1 shows the absorption spectra of azobenzene monolayer before and after photoirradiation on a quartz plate and also in solution. The details of absorption spectra of **1a** on quartz surface and in solution are described in our previous report.[28] The absorption spectra of monolayer of **1b** on quartz surface before the irradiation of 366 nm light shows a strong absorption band at 375 nm which corresponds to the π–π* transition of the substituted *E*-azobenzene. The intensity of the band is decreased upon 366 nm light irradiation and the n–π* transition band around 500 nm was increased. The film reaches its PSS within 40 seconds. On further irradiation with >500 nm wavelength light led to the recovery of the π–π* transition; the system reached another PSS within 240 seconds. These spectral changes can be repeated for many cycles (inset). The similar behaviour of absorption spectra was observed for **1b′** maintaining *tert*-Boc groups in $CH_3CN$ solution which is the typical phenomenon shown between the *E* and *Z* isomerization states of azobenzene derivatives.[46,47] The thermal stability of *Z* isomer of **1b′** in $CH_3CN$ at 22 °C (the temperature at which microtubule motility assay has been done) was also confirmed under dark conditions (inset). Only a very small percentage of *Z* isomer of **1b′** converts into *E* isomer after 1 h and it takes more than 24 h for a complete recovery (Fig. 1, right). Therefore, the contribution of thermal-back reaction can be excluded from our few hour long experiments of the motility assay. Similar photoisomerization changes and thermal stabilities are observed for 10% **1c** or **1d** along with 90% **2a** and **1e** with **2b** on quartz surface and also in corresponding solution of **1b′–e′** upon alternate irradiation of corresponding UV and visible light. After 366 nm light irradiation, the film reaches its PSS within 40 seconds for **1c**, **1d** and **1e**. On further irradiation with corresponding visible light, the film reaches another PSS within 300 seconds for **1c** and **1d** and for **1e** it is 270 seconds. From the spectra, conversion to the *Z* isomer is estimated to be about 40–50% under 366 nm light photostationary state.

In addition to UV-visible absorption spectroscopy measurements, the reversible conformation changes of azobenzene monolayer surface were confirmed by means of contact angle measurements (Fig. 2). The contact angle of monolayer surface of **1a** before irradiation was 65 ± 1°. After UV irradiation it

 

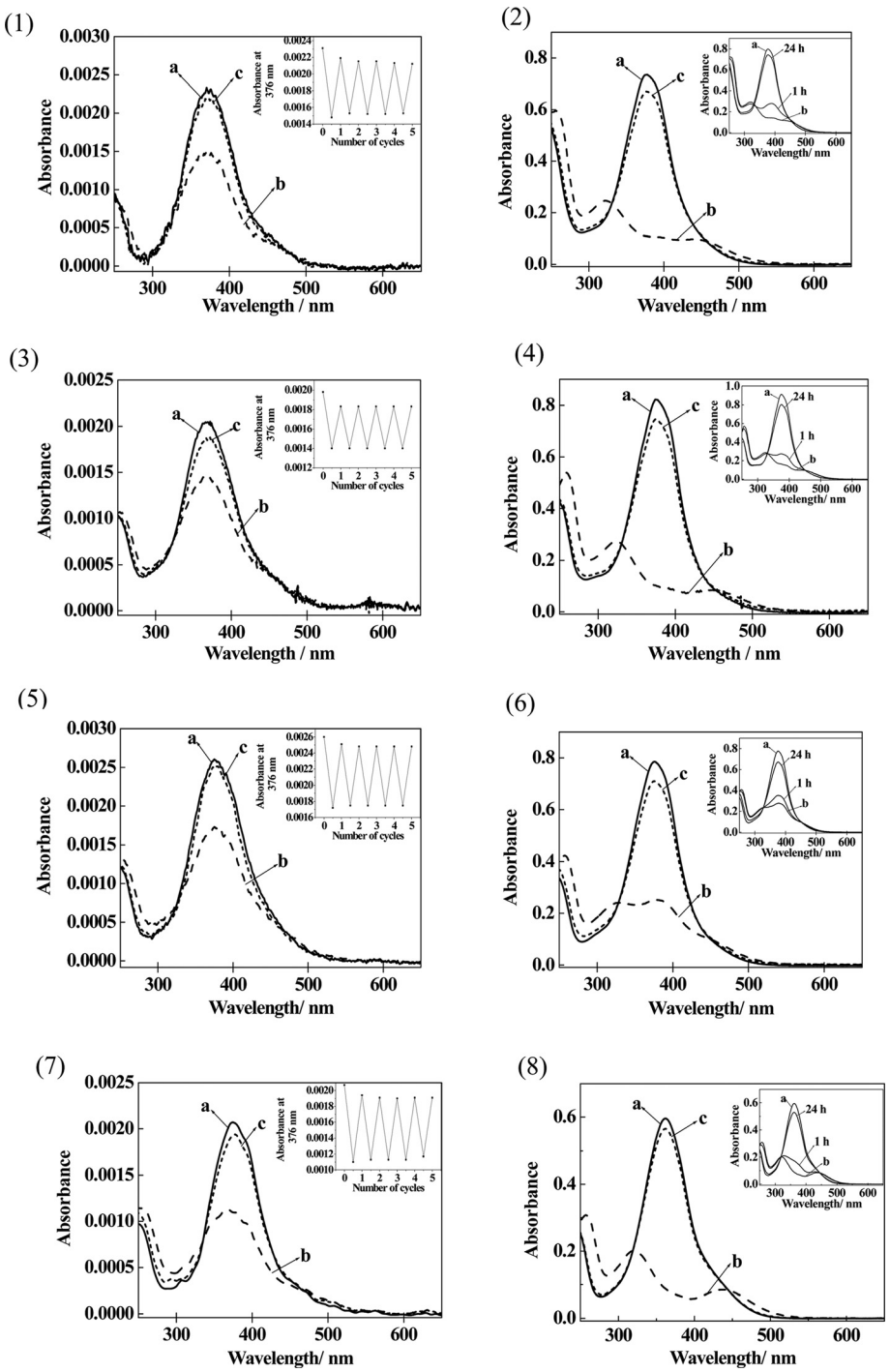


**Fig. 1** Absorption spectral changes of 10% of **1b–e** and 90% of **2a** or **2b** in quartz surface after deprotection of the *tert*-Boc group [left (1), (3), (5), (7)] and that of **1b′–d′** in acetonitrile and **1e′** in DCM before deprotection of the *tert*-Boc group [right (2), (4), (6), (8)]. (a) Before irradiation. (b) Photostationary state (PSS) at 366 nm. (c) PSS at visible light. The inset in the left side shows the absorbance changes at 376 nm after alternating irradiation at 366 nm and visible light over five cycles. The inset in the right side shows the thermal-back relaxation at 22 °C in the dark with the indicated time as well as spectra of pure *E*-isomer (a) and photostationary state under 366 nm light irradiation (b). Smoothing was done to the original spectra of the monolayer to remove spike like noise coming from the instrument.

increased to 69 ± 1°. Regardless of the terminal group, the contact angle was increased after irradiation with 366 nm light irradiation. Monolayers of **1b–e** also showed good reversible photo switching of surface wettability by UV and visible irradiation (data not shown).

The velocity of rhodamine-labelled microtubules on a kinesin-containing surface functionalized with azobenzene derivatives was evaluated with the inverted motility assay.[11] It is already known that in order to get the proper orientation and to avoid inactivation of kinesin, blocking proteins such as casein,

streptavidin, bovine serum albumin are first adsorbed on the substrate.[48–51] But in the present study we systematically removed the blocking proteins and introduced kinesin directly on the photoresponsive azobenzene monolayer. Since there is no blocking protein, we first confirmed the kinesin activity with observable microtubule speed by measuring the average speed of a large population of microtubules. We found that, even though the length of time that the kinesin was catalytically active on the azobenzene monolayers was shorter than that on the corresponding surfaces having blocking proteins, it was sufficiently long enough to perform all of the motility experiments prior to a serious decrease in activity. Next, we investigated the effect of UV light irradiation on the motility of microtubules driven by kinesin in the presence of ATP without functionalized surface. The result shows that the gliding velocities of microtubules with (black circle) and without (triangle) UV irradiation was almost identical (ESI Fig. S2†). This suggested that UV irradiation on a flow cell did not have any detectable effect on the microtubule gliding motility.

In order to know the effect of isomerization of the azobenzene moieties on the motility of rhodamine-labelled microtubules driven by the kinesin-mediated ATP hydrolysis, starting with the azobenzene monolayer in the *E* state, the average gliding velocity of the microtubules was measured. The *Z* rich state of the azobenzene monolayer obtained after 366 nm wavelength light irradiation of flow cell, showed a higher velocity of the microtubule than in the *E* state in **1a–c** and **1e**, making it possible to induce a statistically significant velocity change. Further irradiation of the flow cell with appropriate visible light, the motility of microtubule almost reached its initial state and the velocity increased again upon further irradiation with 366 nm wavelength of light. In contrast, upon alternate irradiation of flow cell of **1d** with UV and visible light, no change was observed in the motility of microtubule. Fig. 3 shows variable and reversible microtubule speeds observed in the gliding assay in four states: prior to irradiation (100% *E*), after irradiation at 366 nm (*Z*-rich), after subsequent irradiation with visible light (*E*-rich) and after subsequent irradiation at 366 nm (*Z*-rich).

**Fig. 2** Reversible switching of contact angle of photoresponsive compound **1a** for water before irradiation (left) and after 366 nm light irradiation (right).

Starting with the flow cell in its *E* isomer rich state and the subsequent irradiation with 366 nm wavelength light, the controllable changes in the velocity of **1a**, **1b** and **1e** was 13–15% of the initial velocity in the *E* form. In the case of **1c** with a glutamic acid residue the speed difference between the *E* and *Z* rich state was found to be about 9%. At the same time **1d** with a malonic acid substituent shows the identical microtubule velocity in *E* and *Z* isomeric forms. In contrast to the results of photoregulation of motility with the deprotected amino acid substituted moieties; no change in the velocity of the microtubules upon photoirradiation was detected for the azobenzene containing the protected amino acid terminal group (Fig. 4).

In our previous report[28] two possible mechanisms were suggested to explain the change in the motility of kinesin–microtubule system upon the photoisomerization of azobenzene monolayer surface. One is that the photoisomerization induced a change in the interaction between the monolayer surface with positively charged amino groups and microtubules being rich in the negatively charged carboxylate groups.[52] The other one is that the photoresponsive monolayer affects the activity of kinesin.

To investigate the influence of azobenzene functionalized monolayer on the activity of kinesin, a microtubule activated

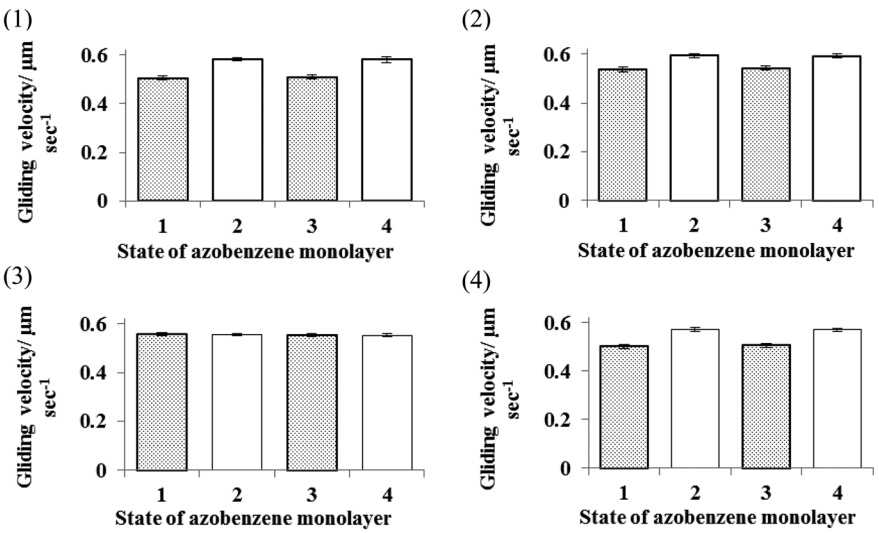


**Fig. 3** Fast and slow mode of microtubule motility upon photoirradiation. (1): **1b**, (2): **1c**, (3): **1d**, (4): **1e**. State 1: Prior to irradiation. State 2: After irradiation at 366 nm. State 3: After subsequent irradiation at visible light. State 4: After subsequent irradiation at 366 nm. The number of microtubules measured was 38, 44, 35, and 30 for **1b**; 40, 35, 37, and 25 for **1c**; 32, 32, 30, and 25 for **1d**; and 46, 41, 43, and 37 for **1e**; for states 1–4, respectively. The error bars indicate the standard error of the mean.

 

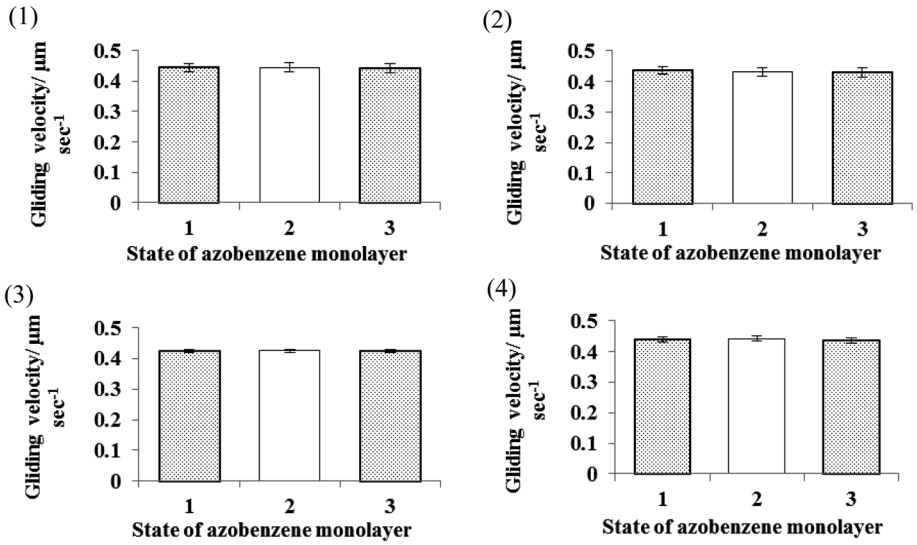


**Fig. 4** Changes in microtubule motility upon photoirradiation of *tert*-Boc protected compounds. (1): **1b′**, (2): **1c′**, (3): **1d′**, (4): **1e′**. The velocity was calculated with the shortest distance of the terminal positions of the microtubule before and after 10 seconds motility. State 1: Prior to irradiation. State 2: After irradiation at 366 nm. State 3: After subsequent irradiation with visible light. The error bars indicate the standard error of the mean.

ATPase assay was performed in the same buffer condition as the motility assay. We determined the rate at which ATP hydrolysis products are formed by using malachite green colorimetric method as explained in the Experimental section. Fig. 5 shows the time dependent inorganic phosphate release from hydrolysis of ATP by kinesin at different states of **1a**. When the azobenzene moiety of **1a** was in *E* form, the initial steady state phosphate release rate was $5.05 \times 10^{-3}$ nmol min$^{-1}$ µl$^{-1}$. Upon UV irradiation of flow cell with 366 nm light about 30 seconds, phosphate release rate was found to be increased to $5.74 \times 10^{-3}$ nmol min$^{-1}$ µl$^{-1}$. The difference in the release rates of phosphate ion between *E* and *Z* isomer was 14% which shows comparable correlation with the gliding velocity of microtubule at two different isomeric surfaces. On further irradiation with >500 nm, the inorganic phosphate release rate reduced to $5.14 \times 10^{-3}$ nmol min$^{-1}$ µl$^{-1}$ and the difference in the release rates between *E* and *Z* isomer was 12%. Similarly, the rate of inorganic phosphate release was switched for **1b–c** and **1e** monolayer surfaces, with similar behaviour as seen in the gliding velocity of microtubule at two different isomeric surfaces (ESI Fig. S3–S6†). In contrast, the release rate of inorganic phosphate in protected azobenzene derivatives upon alternate irradiation with UV and visible light is the same, a striking exact correlation with the microtubule speeds on the two, *E* and *Z*, isomeric states (data not shown).

From the results it is clear that the change in motility of microtubule depends on terminal group of the surface monolayer. When our photoresponsive azobenzene monolayer **1a**, **1b** or **1e** presenting two or more free amino groups with a net positive charge in the buffer solution was used for the inverted motility assay experiment, the gliding velocity of microtubule in the *Z* state was 13–15% higher than the gliding velocity in the *E* state. The azobenzene monolayer surface of **1c** offering one negatively charged carboxyl group and one positively charged amino group gave an increase in microtubule velocity of 9% in the *Z* state than the gliding velocity in the *E* state. In contrast negatively charged surface of **1d** and non-polar surface of protected

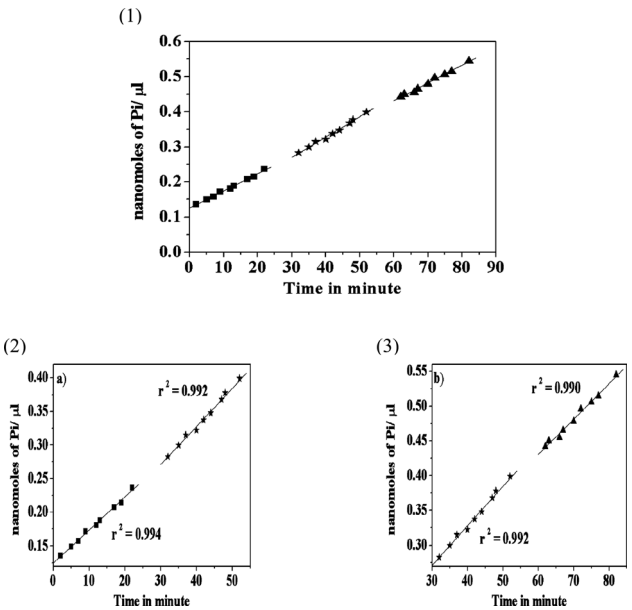


**Fig. 5** Time dependent inorganic phosphate released from hydrolysis of ATP by kinesin in different environments of azobenzene functionalized surface of **1a** before irradiation [(1) squares], after 366 nm irradiation [(1) stars] and after visible light irradiation [(1) triangles]. Enlarged figure of phosphate release before and after 366 nm irradiation (2) and after 366 nm and >500 nm irradiation (3).

monolayer didn't show any change in the gliding velocity between two isomeric forms.

The striking exact correlation between the difference in the gliding velocity of microtubule driven by kinesin and the difference in the rate at which the ATP hydrolysis products formed at two isomeric surfaces, *E* and *Z*, allows us to conclude that the change in the microtubule gliding motility is mainly due to the change in activity of kinesin. It has already been reported that

the activity or the reaction kinetics of kinesin is changed depending on the nature of the surface of the substrate and in some extreme cases, the kinesin is completely inactivated in the absence of a blocking protein on some substrates.[50] Recently Martin *et al.* reported that when the polymer of a hydroxymethylated derivative of EDOT (2,3-dihydrothieno [3,4-*b*][1,4]dioxin–methanol, '$CH_2OH$–EDOT') is electrochemically transformed on the surface from a cationic (doped) state to a neutral (dedoped) state and *vice versa*, the ATPase activity of the adsorbed kinesin can be controlled reversibly, resulting in the reversible control of the gliding speed of the associated microtubule between fast (in the dedoped state) and slow (in the doped state) mode.[53] It is reasonably expected that the terminal amino groups with positive charge dive into the forest of alkyl chain of **2a** or **2b** during *E*-to-*Z* photoisomerization upon 366 nm wavelength light irradiation, which is proved by the increase in contact angle of the monolayer. So when the positively charged amino groups are exposed to the surface at *E* state, the slowdown of microtubule motility is observed and when the alkyl chain is exposed to the surface at *Z* state, the motility of microtubule increased.

The relationship between the kinesin activity and the presence of positive charges on the surface is not clear. The possible mechanism which can explain the change in the kinesin activity and the gliding motility of the microtubule is that the positive charge might have affected the secondary structure of the kinesin, resulting in a change in its activity of ATP hydrolysis.

## Conclusions

We observed that an azobenzene monolayer surface needs to have free amino terminal groups for the dynamic control of the motility of microtubule. The surface of the azobenzene monolayer with terminal amino groups can dynamically control the ATP hydrolysis activity of kinesin which further induces the change in motility of microtubule. We believe that the reported method could facilitate the rational design of new type of photo controllable molecular devices if we could control the motility of microtubule between complete ON/OFF switching. Currently we are trying to find a more suitable terminal group which can completely control the ON/OFF switching of the function of kinesin.

## Acknowledgements

This work was supported by a grant-in-aid for science research in a priority area "New Frontiers in Photochromism (no. 471)" from the Ministry of Education, Culture, Sports, Science, and Technology (MEXT), Japan. M. K. A. R. acknowledges The Ushio Foundation for a scholarship. We thank to Dr Y. Hiratsuka, Dr Y. Hachikubo and Dr T. Q. P. Uyeda for kindly giving recombinant kinesin construct and Dr A. Kakugo, Y. Tamura and Prof. J. P. Gong for help in purification of protein specimen.

## Notes and references

1 A. Agarwal and H. Hess, *Prog. Polym. Sci.*, 2010, **35**, 252–277.
2 A. Goel and V. Vogel, *Nat. Nanotechnol.*, 2008, **3**, 465–475.
3 M. G. L. van den Heuvel and C. Dekker, *Science*, 2007, **317**, 333–336.
4 T. Fischer and H. Hess, *J. Mater. Chem.*, 2007, **17**, 943–951.
5 J. R. Dennis, J. Howard and V. Vogel, *Nanotechnology*, 1999, **10**, 232–236.
6 M. G. L. van den Heuvel, M. P. De Graaff and C. Dekker, *Science*, 2006, **312**, 910–914.
7 L. Ionov, M. Stamm and S. Diez, *Nano Lett.*, 2005, **5**, 1910–1914.
8 K. J. Bohm, J. Beeg, G. M. zu Horste, R. Stracke and E. Unger, *IEEE Trans. Adv. Packag.*, 2005, **28**, 571–576.
9 R. K. Doot, H. Hess and V. Vogel, *Soft Matter*, 2007, **3**, 349–356.
10 R. D. Vale, T. S. Reese and M. P. Sheetz, *Cell*, 1985, **42**, 39–50.
11 J. Howard, A. J. Hudspeth and R. D. Vale, *Nature*, 1989, **342**, 154–158.
12 B. J. Schnapp, T. S. Reese and R. Bechtold, *J. Cell Biol.*, 1992, **119**, 389–399.
13 S. T. Brady, *Nature*, 1985, **317**, 73–75.
14 R. D. Vale, T. S. Reese and M. P. Sheetz, *Cell*, 1985, **42**, 39–50.
15 N. Hirokawa, Y. Noda and Y. Okada, *Curr. Opin. Cell Biol.*, 1998, **10**, 60–73.
16 N. Hirokawa and R. Takemura, *Nat. Rev. Neurosci.*, 2005, **6**, 201–214.
17 R. D. Vale, *Cell*, 2003, **112**, 467–480.
18 D. L. Coy, M. Wagenbach and J. Howard, *J. Biol. Chem.*, 1999, **274**, 3667–3671.
19 S. M. Block, L. S. Goldstein and B. J. Schnapp, *Nature*, 1990, **348**, 348–352.
20 W. O. Hancock and J. Howard, *J. Cell Biol.*, 1998, **140**, 1395–1405.
21 Y. Hiratsuka, T. Tada, K. Oiwa, T. Kanayama and T. Q. P. Uyeda, *Biophys. J.*, 2001, **81**, 1555–1561.
22 M. G. L. van denHeuvel, C. T. Butcher, R. M. M. Smeets, S. Diez and C. Dekker, *Nano Lett.*, 2005, **5**, 1117–1122.
23 M. Platt, G. Muthukrishnan, W. O. Hancock and M. E. Williams, *J. Am. Chem. Soc.*, 2005, **127**, 15686–15687.
24 L. Limberis, J. J. Magda and R. J. Stewart, *Nano Lett.*, 2001, **1**, 277–280.
25 H. Higuchi, E. Muto, Y. Inoue and T. Yanagida, *Proc. Natl. Acad. Sci. U. S. A.*, 1997, **94**, 4395–4400.
26 H. Hess, J. Clemmens, D. Qin, J. Howard and V. Vogel, *Nano Lett.*, 2001, **1**, 235–239.
27 A. Nomura, T. Q. P. Uyeda, N. Yumoto and Y. Tatsu, *Chem. Commun.*, 2006, 3588–3590.
28 M. K. A. Rahim, T. Fukaminato, T. Kamei and N. Tamaoki, *Langmuir*, 2011, **27**, 10347–10350.
29 F. Ercole, T. P. Davis and R. A. Evans, *Polym. Chem.*, 2010, **1**, 37–54.
30 N. Tamaoki and T. Kamei, *J. Photochem. Photobiol., C*, 2010, **11**, 47–61.
31 T. Seki and S. Nagano, *Chem. Lett.*, 2008, **37**, 484–489.
32 S. Yagai and A. Kitamura, *Chem. Soc. Rev.*, 2008, **37**, 1520–1529.
33 K. G. Yager and C. J. Barrett, *J. Photochem. Photobiol., A*, 2006, **182**, 250–261.
34 C. J. Barrett, J. Mamiya, K. G. Yager and T. Ikeda, *Soft Matter*, 2007, **3**, 1249–1261.
35 The following article describes the photocontrol of the ATPase activity of kinesin but not the motility using an azobenzene derivative: M. D. Yamada, Y. Nakajima, H. Maeda and S. Maruta, *J. Biochem.*, 2007, **142**, 691–698.
36 P. Santurri, F. Robbins and R. Stubbings, *Org. Synth.*, 1973, **Coll**. **Vol. 5**, 341; 1960, **40**, 18.
37 F. Cisnetti, R. Ballardini, A. Credi, M. T. Gandolfi, S. Masiero, F. Negri, S. Pieraccini and G. P. Spada, *Chem.–Eur. J.*, 2004, **10**, 2011–2021.
38 K. Aoki, T. Seki, Y. Suzuki, T. Tamaki, A. Hosoki and K. Ichimura, *Langmuir*, 1992, **8**, 1007–1013.
39 M. Dasog, A. Kavianpour, M. F. Paige, H. B. Kraatz and R. W. J. Scott, *Can. J. Chem.*, 2008, **86**, 368–375.
40 M. Castoldi and A. V. Popov, *Protein Expression Purif.*, 2003, **32**, 83–88.
41 H. Suzuki, K. Oiwa, A. Yamada, H. Sakakibara, H. Nakayama and S. Mashiko, *Jpn. J. Appl. Phys.*, 1995, **34**, 3937–3941.
42 J. Howard, A. J. Hunt and S. Baek, *Methods Cell Biol.*, 1993, **39**, 137–147.
43 T. Kodama, K. Fukui and K. Kometani, *J. Biochem.*, 1986, **99**, 1465–1472.
44 H. H. Hess and J. E. Derr, *Anal. Biochem.*, 1975, **63**, 607–613.
45 G. Pace, V. Ferri, C. Grave, M. Elbing, C. von Hanisch, M. Zharnikov, M. Mayor, M. A. Rampi and P. Samori, *Proc. Natl. Acad. Sci. U. S. A.*, 2007, **104**, 9937–9942.
46 K. G. Yager and C. J. Barrett, *J. Photochem. Photobiol., A*, 2006, **182**, 250–261.
47 K. Ichimura, Y. Suzuki, T. Seki, A. Hosoki and K. Aoki, *Langmuir*, 1988, **4**, 1214–1216.

 

48 T. Ozeki, V. Verma, M. Uppalapati, M. Y. Suzuki, M. Nakamura, J. M. Catchmark and W. O. Hancock, *Biophys. J.*, 2009, **96**, 3305–3318.
49 D. J. G. Bakewell and D. V. Nicolau, *Aust. J. Chem.*, 2007, **60**, 314–332.
50 C. Brunner, K. H. Ernst, H. Hess and V. Vogel, *Nanotechnology*, 2004, **15**, S540–S548.
51 E. Berliner, H. K. Mahtani, S. Karki, L. F. Chu, J. E. Cronan and J. Gelles, *J. Biol. Chem.*, 1994, **269**, 8610–8615.
52 D. C. Turner, C. Chang, K. Fang, S. L. Brandow and D. B. Murphy, *Biophys. J.*, 1995, **69**, 2782–2789.
53 B. D. Martin, L. M. Velea, C. M. Soto, C. M. Whitaker, B. P. Gaber and B. Ratna, *Nanotechnology*, 2007, **18**, 055103.